machines

Review

Utilization of Additive Manufacturing in the Thermal Design of Electrical Machines: A Review

Martin Sarap [1,*], Ants Kallaste [1], Payam Shams Ghahfarokhi [1,2], Hans Tiismus [1] and Toomas Vaimann [1]

[1] Department of Electrical Power Engineering and Mechatronics, Tallinn University of Technology, 19086 Tallinn, Estonia; ants.kallaste@taltech.ee (A.K.); payam.shams@taltech.ee (P.S.G.); hans.tiismus@taltech.ee (H.T.); toomas.vaimann@taltech.ee (T.V.)

[2] Department of Electrical Machines and Apparatus, Riga Technical University, Kaļķu iela 1, LV-1658 Riga, Latvia

* Correspondence: martin.sarap1@taltech.ee

Abstract: Additive manufacturing (AM) is a key technology for advancing many fields, including electrical machines. It offers unparalleled design freedom together with low material waste and fast prototyping, which is why it has become to focus of many researchers. For electrical machines, AM allows the production of designs with optimized mechanical, electromagnetic and thermal parameters. This paper attempts to give the reader an overview of the existing research and thermal solutions which have been realized with the use of AM. These include novel heat sink and heat exchanger designs, solutions for cooling the machine windings directly, and additively manufactured hollow windings. Some solutions such as heat pipes, which have been produced with AM but not used to cool electrical machines, are also discussed, as these are used in conventional designs and will certainly be used for additively manufactured electrical machines in the future.

Keywords: additive manufacturing; electrical machines; metal 3D-printing; electrical machine cooling

Citation: Sarap, M.; Kallaste, A.; Shams Ghahfarokhi, P.; Tiismus, H.; Vaimann, T. Utilization of Additive Manufacturing in the Thermal Design of Electrical Machines: A Review. *Machines* **2022**, *10*, 251. https://doi.org/10.3390/machines10040251

Academic Editor: César M. A. Vasques

Received: 1 March 2022
Accepted: 25 March 2022
Published: 31 March 2022

1. Introduction

The basic design philosophy of electrical machines has remained relatively unchanged for many years, as it has been constrained by the available manufacturing methods. With the rising demand for electric vehicles and green energy, there is a significant push towards higher efficiencies, power densities, lighter weights, and customized solutions for electrical machines, meaning that innovation in the field is required. One technology that might meet those demands is additive manufacturing (AM).

AM, known in the consumer space as 3D printing, is a technology with the ability to manufacture practically any object for which a 3D model can be created, without the complexity and specific geometry of the part significantly impacting the manufacturing costs. This provides huge amounts of design freedom to engineers, who can fully leverage modern computational tools to create truly optimal designs without being constrained by the manufacturing method. Modern AM technologies can utilize many different types of materials, from flexible polymers to high-performance metals, and the local manufacturing nature of AM makes it less reliant on global supply chains. These advantages, in addition to the rapid prototyping and low material waste capabilities, have ensured rapid growth in the field of AM: per the 2021 Wohlers Report, the industry grew by 7.5%, reaching a value of $12.8 billion in 2020 [1]. The largest shares of that are the medical, dental, and aerospace industries which are forecasted to help the AM market reach a value of $51 billion by 2030 [2].

With increased power densities and more demanding requirements, the thermal design of machines becomes more important, as larger amounts of heat need to be extracted from smaller-sized machines. AM provides many novel solutions which can be used to enhance the thermal performance of an electrical machine. For air-cooled machines, traditional radiator fins can be replaced with complex shapes. These can be integrated into the machine to provide structural support while being optimized for minimal weight. For water-cooled machines, the coolant paths can be more complex [3] and brought closer to the heat generation [4].

Therefore, the aim of this paper is to give the reader a summary of the current progress in the utilization of AM in the thermal design of electrical machines. The relevant AM methods, together with their capabilities and limitations, are described to provide an overview of the different technologies and materials used. The paper focuses on different solutions which have taken advantage of the manufacturing freedom offered by AM and can be used to improve the thermal capabilities of existing electrical machines or to manufacture new optimized machines.

2. Additive Manufacturing

Current AM methods can be classified into seven main categories: vat photopolymerization, material extrusion, material jetting, binder jetting, powder bed fusion (PBF), direct energy deposition, and sheet lamination [5,6]. Each method creates the three-dimensional object in a different way and has its own advantages and disadvantages. The biggest differences are in the available materials as photopolymerization and extrusion processes utilize mostly plastic materials, whereas metal objects are most often manufactured with PBF methods.

AM started off in 1987 with the emergence of stereolithography (SLA) [7], which is a vat polymerization technology. This method consists of solidifying thin layers of light-sensitive liquid polymers with a UV light source (Figure 1a), which in the original case was a laser. The position of the laser beam can be accurately controlled using a mirror galvanometer system, resulting in extremely detailed parts. Modern consumer machines often use a UV LED array together with a high-resolution LCD photomask to reduce cost and complexity. This generally produces less detailed parts but has the benefit of being able to print the entire layer at the same time, which significantly improves the printing speed. While only the polymer can be directly hardened, other materials can be added into the liquid polymers as powders. After manufacturing, the hardened polymer can be burned away, leaving only the added material behind, although heavily shrunk compared to the original printed part. This allows SLA to be used for the manufacturing of ceramic and metal parts.

In 1991, fused deposition modeling (FDM) was commercialized with the launch of Stratasys's first FDM printer [8]. With this technology, individual layers are constructed by precisely extruding thermoplastic materials according to a CAD model (Figure 1b). The low costs associated with FDM machines and materials have made it by far the most popular consumer AM technology [9]. The material selection for FDM is wide, as many thermoplastics can be successfully printed, and similarly to SLA, other materials can be used as fillers. Furthermore, fully metal-based solutions based on material extrusion have recently become available [10].

The AM method with the widest material selection is binder jetting (BJ) [11], where an inkjet mechanism is used to selectively deposit a binder material into the powdered material to form layers. BJ can utilize many types of materials, such as ceramics, metals, and polymers. Full-colored prints are also possible due to the inkjet mechanism. The method allows for large build areas, as the binder solidifies at room temperature and does not introduce warping. Depending on the material, the printed parts need to be sintered or infiltrated with a low melting-temperature metal [12]. This produces a part with significant internal porosity, potentially making the method unsuitable for applications where demanding material properties are required.

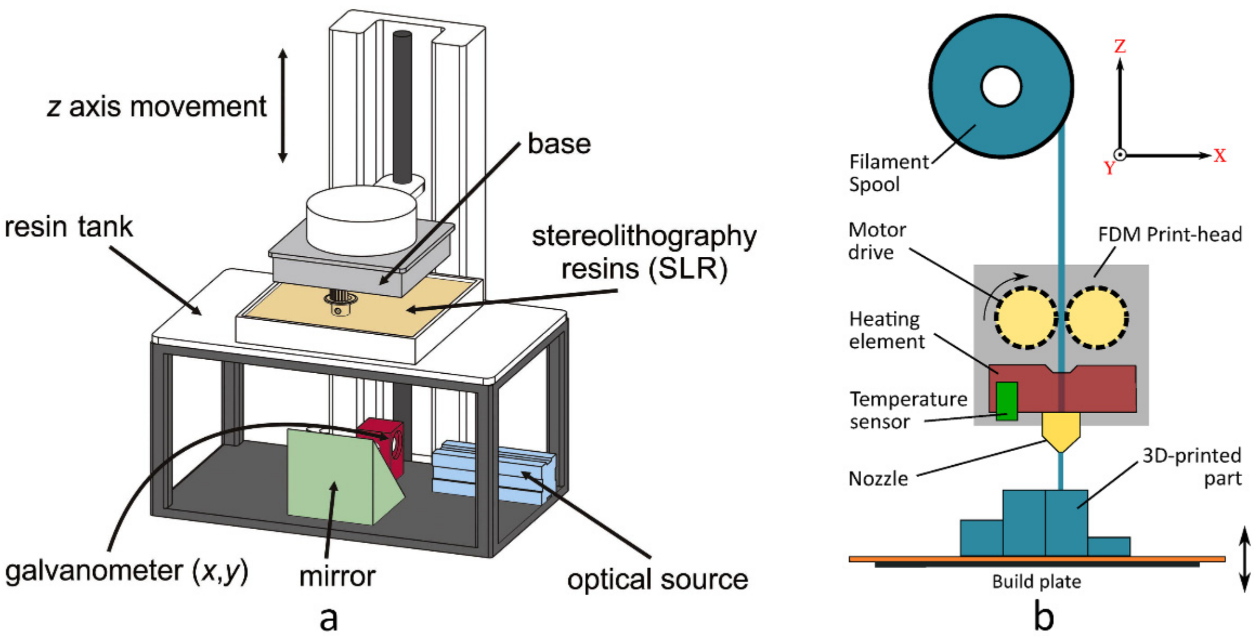

Figure 1. Schematics of (**a**) SLA reprinted with permission from Ref. [13]. Copyright 2016 Elsevier and (**b**) FDM [14] processes.

The first powder bed fusion (PBF) method called selective laser sintering (SLS) became available in 1992 [7], although it was patented several years earlier [15]. SLS involves using a powerful laser to selectively fuse powder particles into layers. After each layer, the build platform is lowered, a new coat of powder is applied, and the process repeats until the part is ready. The process of a general laser powder bed fusion (L-PBF) is illustrated in Figure 2. The thickness of each coat of powder defines the layer thickness and determines the Z-axis accuracy of the part. The X- and Y-axis accuracy is determined by the laser assembly and material used. It can be used to manufacture parts from many different types of materials, even metals and ceramics, and can print without the use of support structures, as the part can be supported by the unsintered powder in the build chamber. The technology of selective laser melting (SLM), which was started in 1995 [16], is similar to SLS, as it is also a powder bed process. However, instead of sintering, the (metal) powder is completely melted, leading to a less porous and more homogeneous part with improved thermal, electrical, and magnetic properties. A natural evolution of SLM is the technology of electron beam melting (EBM), where an electron beam is used instead of a laser. This allows for higher energy densities and a wider selection of materials. When printing metals, a dimensional tolerance of ±0.1 mm is often cited [17], and with SLM and EBM, densities over 99% can be achieved [18,19].

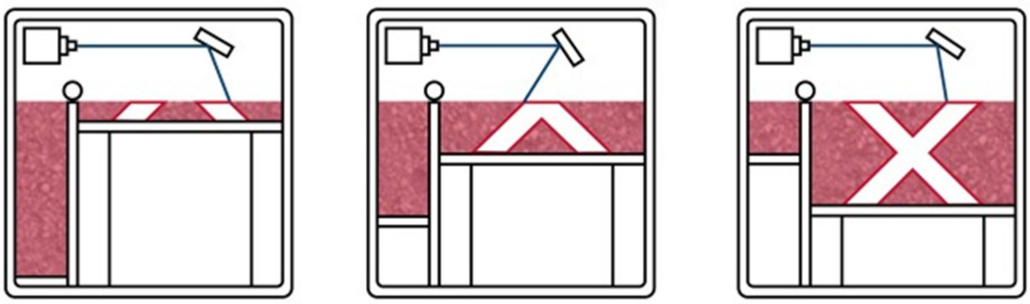

Figure 2. Schematic of a laser powder bed fusion process [20].

2.1. Materials Used in AM

AM allows many different materials to be used. In the context of thermal solutions for electrical machines, the relevant materials are either good electrical conductors, dielectrics, or have good magnetic properties. These materials are used for different purposes but for all of them, a high value of thermal conductivity is beneficial for increasing the total thermal performance of the machine.

The windings of an electrical machine need to be highly electrically conductive, meaning that copper is an ideal choice. AM allows the shape of the conductors to be optimized for both electrical and thermal purposes. However, a significant challenge in the additive manufacturing of machine windings is the relative difficulty of printing fully dense copper with a PBF based process, as copper reflects up to 98% of the energy applied by an infrared laser beam often used in SLM [21]. This problem can be mitigated by using a green laser [22] or an electron beam [23,24] to achieve virtually fully dense parts with physical properties equivalent to the solid material. Copper can also be printed with other AM methods, such as BJ, SLA, and FDM, but due to the internal porosity of the final part, the thermal conductivity of the resulting object is lower [25,26].

Even though printing copper is less common due to the technological requirements, some impressive results have been achieved. Simpson et al. [27] have used DMLS to create copper alloy windings that are shaped for minimal AC losses (Figure 3a). The experimental results show reduced AC losses, although the electrical conductivity of the sintered material is only 51% IACS. A higher conductivity value of 90% IACS [28] has been achieved by using SLM and a copper alloy (CuCr1Zr) to create an induction heater with integrated water cooling (Figure 3b). The copper alloy CuCr1Zr is noteworthy, as it can be successfully manufactured using SLM with an infrared laser, while still having high thermal (310–340 W/m/K) and electrical (≥43 MS/m) conductivity [29,30]. The primary alternative to copper is usually aluminum, with the alloy AlSi10Mg receiving the most attention in AM [31].

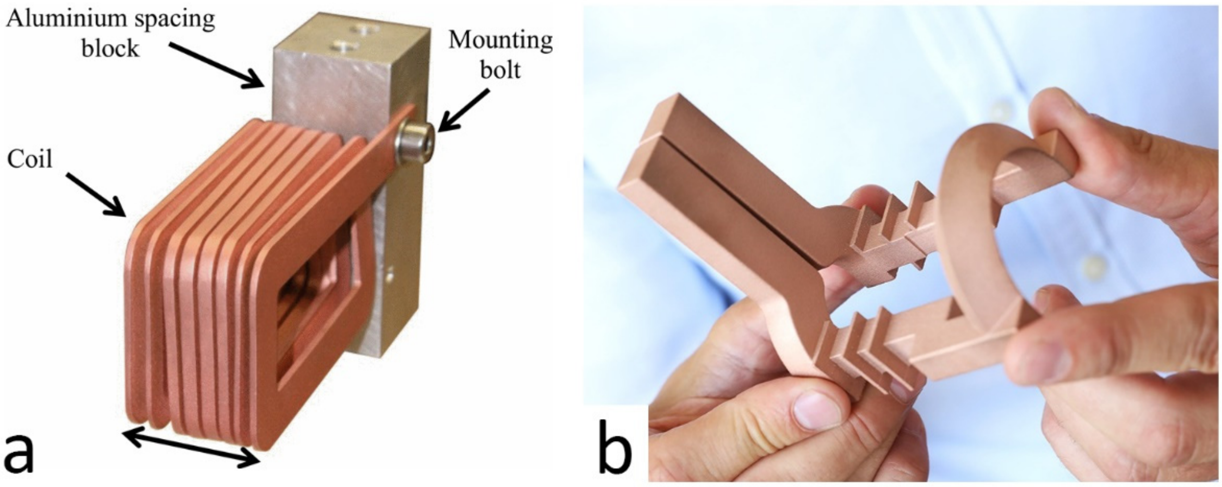

Figure 3. Additively manufactured (**a**) copper alloy windings [27] and (**b**) an induction heater with integrated water cooling [28].

The printing of soft magnetic materials allows for the geometry of the core of an electrical machine to be optimized. This may include liquid cooling channels inside the iron core or cooling fins on the stator surface. The ability to integrate the cooling elements with the machine's core can be beneficial due to the elimination of any contact thermal resistance, even if the thermal conductivity of soft magnetic materials is relatively low. The materials used are typically ferrosilicon alloys, which can be successfully printed using PBF and other AM methods.

The dielectric material needed to insulate the conductive windings is often a large source of thermal resistance in an electrical machine, as the electrically isolating materials used in machines are also poor thermal conductors (values of around 1 W/m/K). This is not the case with some ceramics, which through the use of AM could be utilized in electrical machines as thermally conductive isolation material. Several different AM methods can utilize ceramic materials, including SLA, by suspending the ceramic powder inside a liquid photopolymer [32]. For example, Rauchenecker et al. [33] were able to create complex-shaped alumina nitride ceramic parts with thermal conductivity values over 160 W/m/K. The thermal conductivities of some popular materials manufactured with different AM methods are presented in Table 1.

Table 1. Thermal conductivities of popular materials used in AM.

Material	Manufacturing Method	Effective Thermal Conductivity (W/m/K)
Pure copper	Electrolysis	394
	EBM	390 [34]
	SLM	317–336 [25]
	BJ	245–327 [25]
	Extruded paste	284 [35]
CuCr1Zr	Cast	310–340 [30]
	SLM	309 [36]
AlSi10Mg	Cast	113 [37]
	SLM	173 [38]
	SLS	100 [39]
Electrical steel	SLM	26 (Fe-3.7 w.t.% Si) [40]
Alumina nitride ceramic	Pure	285 [41]
	SLA	>160 [33]
	BJ	3–4 [42]
Alumina ceramic	SLA	35 [43]

2.2. Additively Manufactured Electrical Machines

In the realm of electrical machines, AM is still in the research stage. Individual components of an electrical machine have been successfully manufactured by several groups. Urbanek et al. [44] have designed and manufactured a PMSM rotor from a soft-magnetic ferro-silicon alloy using a laser PBF process. The rotor is designed to utilize the advantages provided by AM by incorporating several design optimizations, including a skewed active part and a hollow shaft. Tseng et al. [45] have used SLM to create a novel SRM rotor that incorporates skewing to reduce cogging torque and plastic ribs to reduce windage losses. Ibrahim et al. [46] have used cold spray AM to create a rotor with alternative PM and soft magnetic composite material layers. The use of AM allowed them to eliminate the bridges and center-posts normally present in PMSM rotors, which limit the motor capabilities.

Some groups have used AM to produce working electrical machines, although not all parts were printed. Tiismus et al. [47] have used SLM to create a working axial-flux switched reluctance motor (Figure 4a). It includes a stator and a rotor which were manufactured from silicon steel. Wu et al. [48] have designed and printed a fan motor that includes a rotor with an integrated impeller to achieve a robust motor with an improved power density (Figure 4b). Ge et al. [49] have used SLA and metal plating to create an electrostatic motor (Figure 4c).

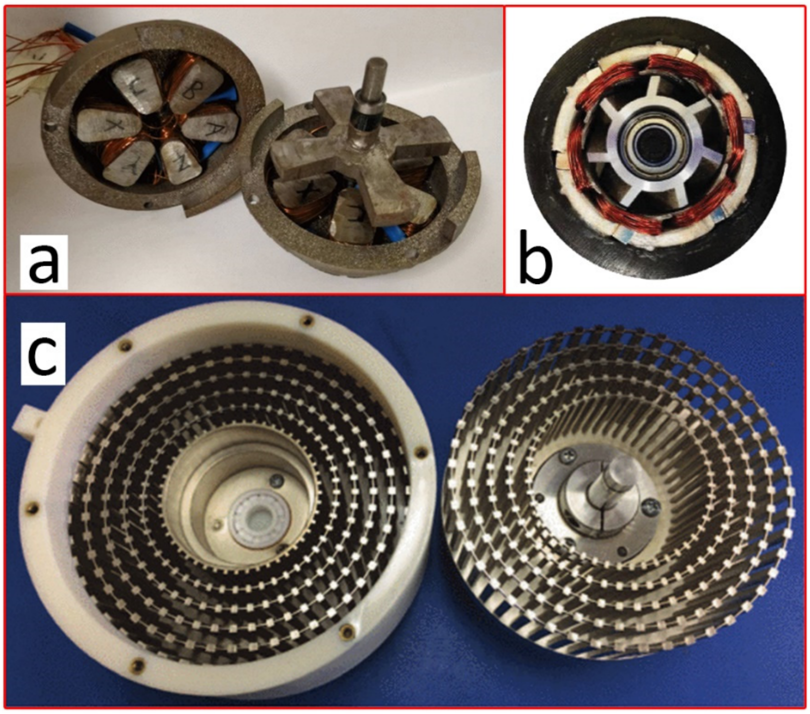

Figure 4. Additively manufactured electrical machines: (**a**) axial flux motor [47], (**b**) integrated fan motor reprinted with permission from Ref. [48]. Copyright 2021 Elsevier, (**c**) electrostatic motor [49].

A completely additively manufactured electrical machine, where the windings, insulation, and soft magnetic materials are all printed concurrently, has not yet been achieved, as this would need advances in multi-material printing technologies. Powder bed fusion processes can generally only print a single material, although dual-metal systems do exist [50]. Nonetheless, research in the area is going strong, as additively manufactured electrical machines can have many advantages over traditionally manufactured counterparts [51].

3. Additively Manufactured Thermal Management Solutions for Electrical Machines

The thermal management of electrical machines is the main challenge with higher power densities due to the increased heat generated in the windings and core. Higher temperatures are detrimental to the machine's efficiency and reliability, meaning that increases in power density are accompanied by a demand for more powerful cooling. The thermal management methods for electrical machines can be categorized into two main groups—air and liquid cooling (Figure 5). For less power-dense machines, air cooling is often sufficient, and in the case of passive air cooling, the necessary airflow is generated only by natural convection. Liquid cooling is used for more demanding applications and can be further divided into direct and indirect liquid cooling, based on the proximity of the coolant fluid to the source of heat. The most common method of liquid cooling utilizes a cooling jacket, which is a casing with coolant channels that surrounds the machine. Direct liquid cooling methods increase performance by bringing the coolant closer to the source of heat.

Several additively manufactured solutions, which could be used to enhance the performance of most of these methods, have been researched, although only a few examples of AM being used to cool electrical machines specifically currently exist in the literature. This means that there are many opportunities for researchers to utilize existing AM solutions for the cooling of electrical machines. Furthermore, AM can provide novel cooling solutions, which are not practical to manufacture using traditional methods and therefore have previously not received substantial attention.

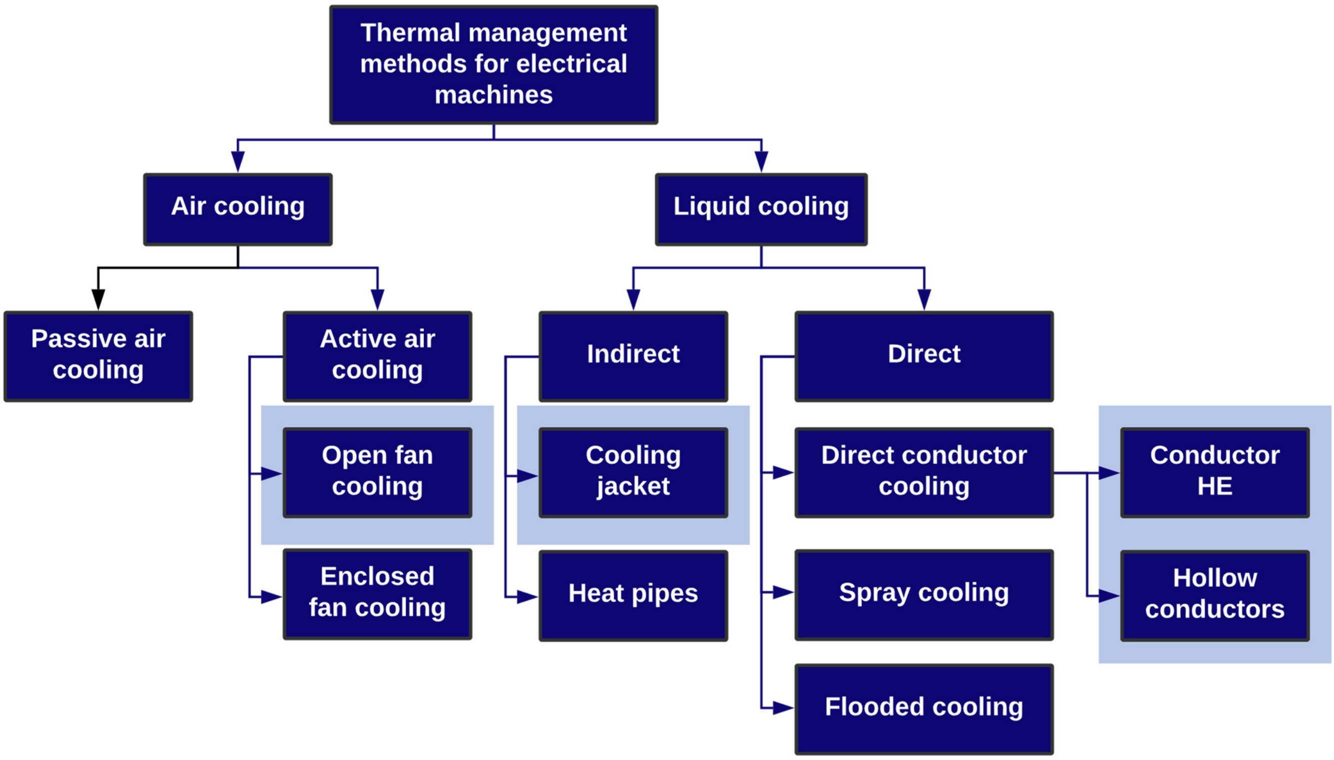

Figure 5. Various cooling methods for electrical machines. The light blue shading indicates that an additively manufactured solution for an electrical machine exists in the literature.

3.1. Air Cooling

The simplest way of cooling an electrical machine is through air cooling. The thermal performance of an air cooler depends on its surface area and the velocity of air interacting with that area, with increased surface areas and air speeds resulting in higher cooling capabilities. Air-cooled electrical machines usually incorporate fins on the body to increase the total surface area, which enhances the cooling by increasing the total convective heat transfer rate of the motor body. Using traditional manufacturing techniques (extrusion, skiving, die-casting, and machining) severely limits the shape and dimensions of the cooling fins, as complex shaped fins would be too costly or even impossible to produce. This is not a concern with additive manufacturing, as any shape can be produced, and the cost of a part does not depend on its complexity, meaning that thermally optimal designs can be manufactured.

The simplest air-cooled machines utilize passive cooling, which means that all of the airflow is generated through natural convection. This increases reliability due to a lack of moving parts but creates a complicated design challenge. Simply increasing the cooling surface area can restrict the airflow in the fin structure to the point of lowering total performance. The optimal solution where the surface area and the airflow created by natural convection are both maximized is highly non-trivial and requires advanced methods such as topology optimization (TO).

TO is a mathematical method that spatially optimizes the distribution of material within a defined domain by fulfilling given constraints previously established and minimizing a predefined cost function [52]. For electrical machines, topology optimization has mainly been used to optimize the electromagnetic and mechanical design [53], while thermal optimization has received little attention. The shapes generated by topology optimization with typical thermal constraints are often too complex to produce with traditional methods [54] and thus need additional constraints to produce practical results. However, in the case of AM, these constraints are not required, as practically any shape can be manufactured (although some constraints may still be beneficial for increased printing success [55]). For this reason, topology optimization is widely used in AM [56–59].

Lazarov et al. [60] have used AM to create several different passive heatsinks and have compared different design ideas—TO, lattice structures, and pin fin. The heatsinks were all manufactured from an aluminum alloy, and the designs incorporate the same dimensional limitations. Out of the designs tested, the clear winner was the TO variant, which performed significantly better than any lattice structured design, even though it has a significantly smaller surface area. The difference in performance is explained by the increased airflow that the optimized design can generate through natural convection. The results of the tests are presented in Figure 6. It should be noted that the optimization was performed in a horizontal orientation. The researchers used the TO design to create a simplified and cheap to produce pin fin design, which also performed better than the lattice designs in the horizontal orientation. This research shows the benefits of TO and that simply increasing the surface area with a lattice structure is not necessarily optimal.

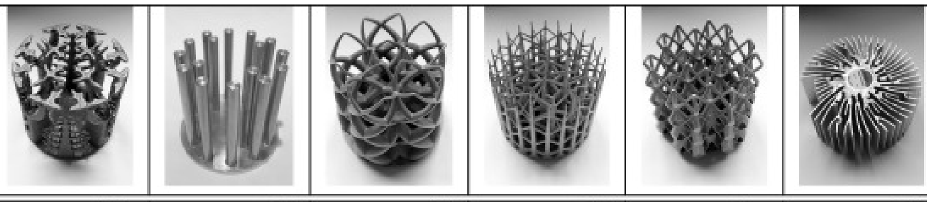

	TO	PF	AT	BT	CT	DT
Mass [g]	98	96	119	116	117	205
Volume V [$\times 10^{-5}$m^3]	3.94	3.53	4.46	4.39	4.46	7.37
Surface A [$\times 10^{-2}$m^2]	2.36	2.22	2.55	4.19	4.18	10.53
$f = A/V$ [$\times 10^2$m^{-1}]	6.00	6.30	5.72	9.55	9.30	14.30
Power	Horizontal orientation Δt [°C]					
1.09W	**5.30**	6.45	6.71	6.93	7.38	5.62
2.96W	**12.41**	15.25	16.16	15.63	16.51	13.23
5.27W	**19.59**	24.12	25.66	25.02	26.10	21.50
	Vertical orientation Δt [°C]					
1.09W	5.32	6.69	6.81	6.00	6.60	5.52
2.96W	12.71	16.54	16.32	14.19	14.80	12.33
5.27W	20.62	26.98	25.96	22.09	23.56	19.01

Figure 6. Topology optimized additively manufactured heat sink compared to conventional designs [60].

The advantages of AM for passive air cooling are further demonstrated by Wits et al. [61], who have taken a bio-inspired design approach to create heatsink designs, which are initially based on naturally occurring brain corals (Figure 7a). They have created structures and optimized the design parameters using computational fluid dynamics to manufacture several heatsinks from an aluminum alloy (AlSi10Mg) using SLM. The design succeeds in promoting natural convection (Figure 7b) while still having a high total surface area. Although the authors note that the simulations show decreased surface heat flux in the middle part of the heatsink fins, meaning that the design could be further optimized to increase the effect of natural convection inside the fin structure.

Air-cooled electrical machines with higher power densities require the use of fans as relying only on natural convection is insufficient. While maximizing surface area is still relevant, the goal of aiding natural convection is replaced with the challenge of reducing pressure drop over the fin structure as a higher pressure drop lowers the airflow acting on the fins. A common way of increasing the surface area of an AM heat sink is through the use of lattice structures, which are a form of cellular structure defined as a spacefilling unit cell that can be tessellated along any axis with no gaps between cells [62]. These structures have been traditionally used to reduce weight while retaining necessary mechanical properties.

With the advent of AM, it has become possible to create arbitrary structures from many different materials. Due to this, there has been significant research in the thermal and mechanical properties of additively manufactured lattice structures [63–66].

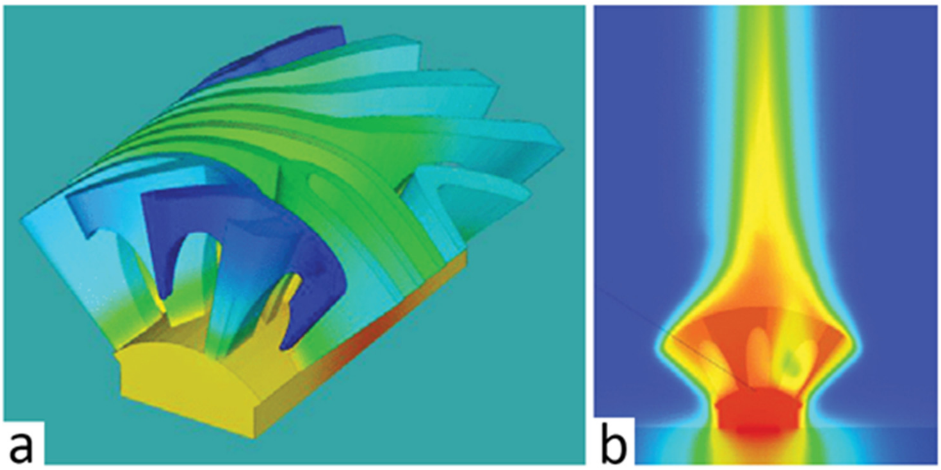

Figure 7. Simulated temperature (**a**) and airflow (**b**) of the passive heat sink with freeform geometry reprinted with permission from Ref. [61]. Copyright 2018 Elsevier.

For thermal solutions, lattice structures can be used to increase the working surface area of a heatsink while keeping the volume constant. Naively one might create an incredibly dense mesh (lattices with a unit cell size of under 1 mm and a strut diameter of 0.1 mm have been achieved with PBF [67]) and achieve a huge surface area, only to find that such a heatsink does not match expectations, as the increased air resistance created by the dense mesh more than cancels out the effects of the higher surface area. One example of this was observed here [68], as a heatsink with 31% more surface area performed worse than a traditional finned design. Although this does not mean that lattice structures should not be considered for heatsinks. Their ability to provide structural support while having a low weight could outweigh the subpar thermal performance. Furthermore, for electrical machine applications, lattice structures can be beneficial for reducing eddy current losses.

Wong et al. [69] have created several heatsinks from aluminum 6061 using SLM (Figure 8). These include two conventional designs—cylindrical pin (a), rectangular fin (b), and three novel designs—a rectangular fin array with rounded corners (c), a staggered elliptical array (d), and a lattice structure (e and f). The novel heatsink designs are only suitable for AM due to the fine detail and compact spacing of the pin fins, which would make conventional manufacturing prohibitively expensive. They investigated the thermal and fluid flow characteristics of the heatsinks and found that the elliptical pins outperformed their conventional counterparts in both heat extraction and pressure drop, as their shape creates a large surface area while keeping air resistance low. One of the worst performers was the lattice structure, which has a very large surface area but presented too large of a pressure drop to perform effectively. Even though the heatsinks investigated in this study were not fully optimized, they clearly demonstrated the performance enhancements that SLM can provide.

AM also allows designers to utilize fin geometries which can provide structural support while being optimized for lower weight. Wrobel et al. [70] have used AM to create an air-cooled aluminum alloy (AlSi10Mg) heat exchanger (HE) for a propulsion motor in a solar aircraft (Figure 9). The HE needs to cool the motor during take-off, when the losses are the highest, while being lightweight for cruising efficiency and providing structural support to the motor. It is integrated into the motor design, as this allows it to be directly connected to the stator teeth, such that the thermal resistance between the heat generating windings and the HE fins is minimized. The design takes full advantage of AM by utilizing curved fins to maximize the surface area while keeping the weight low.

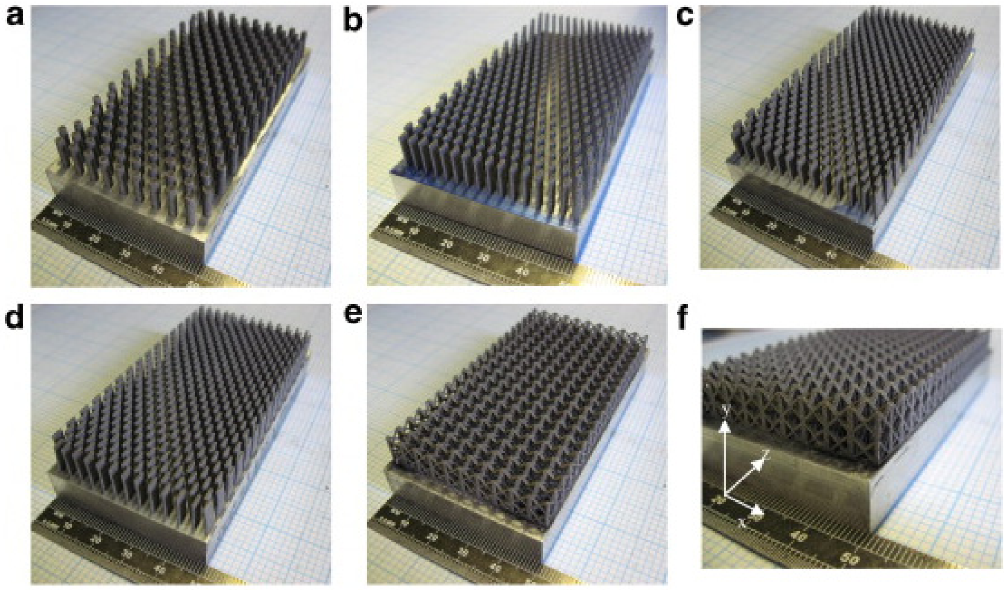

Figure 8. Additively manufactured pin fin heat sinks with different geometries: cylindrical pin (**a**), rectangular fin (**b**), rectangular fins with rounded corners (**c**), staggered elliptical array (**d**) and a lattice structure (**e**,**f**) Reprinted with permission from Ref. [69]. Copyright 2009 Elsevier.

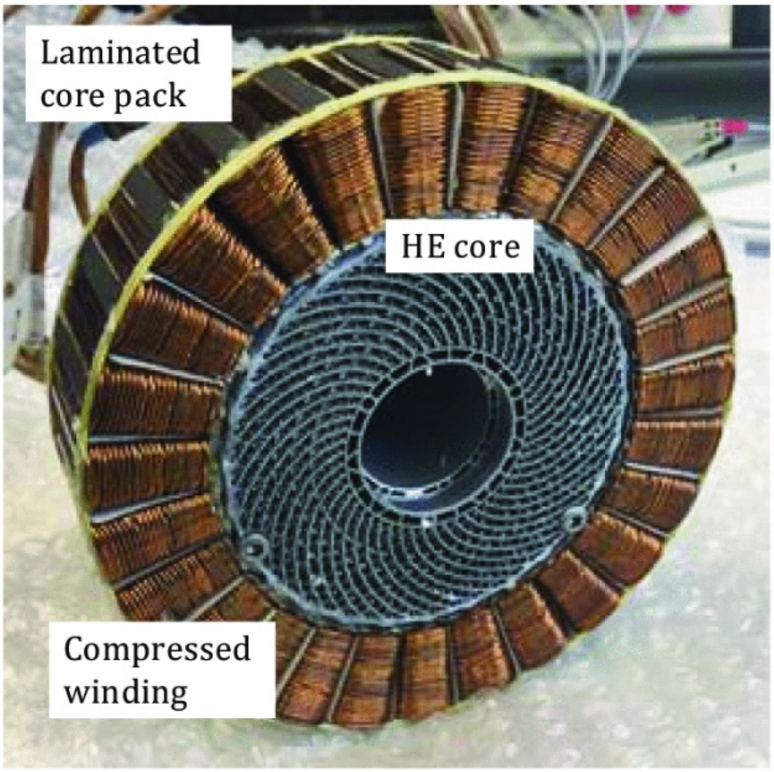

Figure 9. Additively manufactured aluminum alloy heat exchanger for a propulsion motor [70].

While traditional heat sink fins are relatively smooth and flat due to the manufacturing methods, a heat sink produced with AM can easily include patterns and shapes on the fin surfaces, which increases cooling performance. Rao et al. [71] have researched heatsink fins with dimpled surfaces, and they calculated that a surface with teardrop dimples shows 1.8 to 2 times better heat-transfer enhancement compared to a flat plate.

Although adding a surface pattern might not be necessary, as the additively manufactured metal has inherently rough surfaces that can be beneficial for cooling (Figure 10).

Ventola et al. [72] have measured parts manufactured by direct metal laser sintering and found an up to 73% increase in cooling performance over similar smooth parts. The authors explain that as these results are not explained by the increased surface area due to the roughness, the performance must be caused by turbulent flows created by the multi-scale roughness. They suggest a novel method of modelling this effect, which is in excellent agreement with their measured results. As tools to optimize surface roughness become available, designers of additively manufactured machines may start to use them to vary the printing parameters in certain parts of the machine to achieve optimal cooling performance. The effects of surface roughness were also studied by Kirsch et al. [73], who created several microchannel pin fin arrays using L-PBF. It was found that the surface roughness of pins can be beneficial by exacerbating pin wake interactions. The authors also noted that pin spacing could be increased without sacrificing thermal performance, meaning that the weight and material costs of heat exchangers could be decreased with the use of AM.

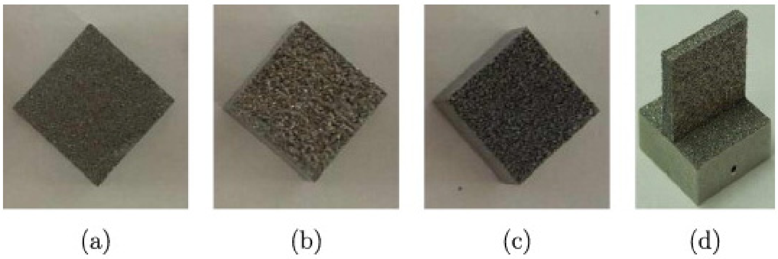

Figure 10. Aluminum alloy samples manufactured using DMLS with different average surface roughness: 16 µm (**a**), 24 µm (**b**), 43 µm (**c**), 22 µm (**d**) [72].

3.2. Liquid Cooling

In the case where air cooling is insufficient, liquid cooling can be used to increase the thermal performance of an electrical machine. This is commonly achieved through a water jacket around the machine body, where the heat from the stator is extracted by the coolant. If the cooling jacket is separate from the stator, the contact resistance between the stator surface and the cooling channels significantly reduces thermal performance. The alternative solution is to integrate the cooling channels in the stator design, although this is difficult with conventional manufacturing methods. With an AM motor, optimized coolant paths can be freely integrated into the core, allowing for greatly improved thermal performance. AM can also improve the thermal capabilities of an existing motor by printing a separate cooling jacket with a geometry that is optimized for a specific design. Two examples of this is an aluminum cooling jacket [74] for an electric racing car which increased performance by 37% compared to the previous version (Figure 11a), and a liquid-cooled casing for an electric motor [75] which produced a 10% weight saving and a 30% reduction in size (Figure 11b).

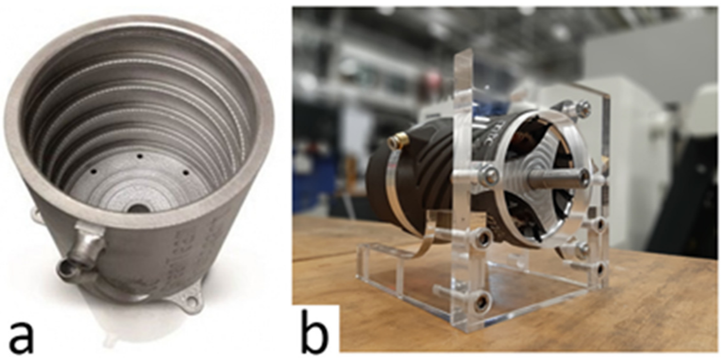

Figure 11. Additively manufactured cooling jackets (**a**) [74] and (**b**) [75].

The thermal performance of a liquid-cooled electrical machine is heavily dependent on the rate of heat exchange from the machine body to the coolant. Similarly to air cooling, this depends on both the surface area and the pressure drop. Due to the complex nature of fluid dynamics, this optimization is highly non-trivial and often results in solutions that cannot be manufactured using traditional methods. This makes heat exchangers one of the more popular thermal devices to take advantage of the capabilities of metal AM. The ability to produce monolithic parts with high levels of geometric complexity, intricate internal structures, and thin walls lends itself perfectly to creating optimized heat exchangers [76,77].

Moon et al. [78] have created an additively manufactured aluminum alloy (AlSi10Mg) HE (Figure 12). The design incorporates a complex fin structure that takes full advantage of AM, achieving a 4X improvement in power density compared to conventional designs. Bernardin et al. [79] have used Direct Metal Laser Sintering (DMLS) to create a stainless-steel twisted tube HE. Utilizing a twisted shape is a known technique for increasing the working surface area and thus the overall heat transfer coefficient of a HE without increasing its size, but the increased manufacturing cost compared to a straight tubed design has suppressed its popularity. For AM, the complexity of the part has little effect on the final cost, meaning that these kinds of optimized designs can be widely used.

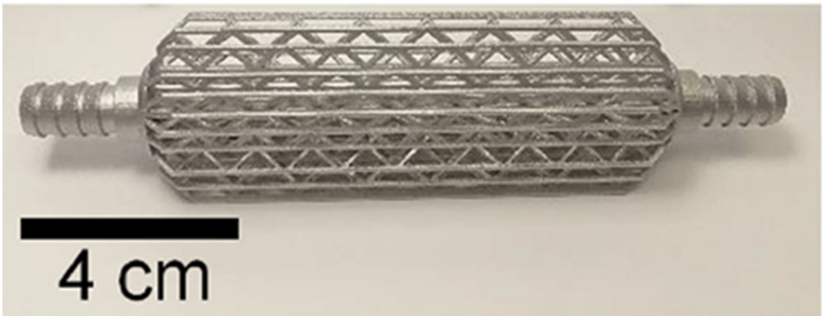

Figure 12. Additively manufactured heat exchangers: a design with a complex fin structure reprinted with permission from Ref. [78]. Copyright 2020 Elsevier.

3.3. Phase Change Cooling

The thermal performance of an electrical machine can also be increased by utilizing heat pipes [80]. These are relatively simple devices that use phase transitions to achieve high values of thermal conductivity [81]. The design of a heat pipe relies on capillary pumping by the wicked interior surface of the device. As it is possible to produce such a surface with AM, there has been significant research in the utilization of different AM methods to produce heat pipes. SLM has been used to create heat pipes from Ti-6Al-4V [82], AISI 316 [83], AlSi12 [84] (Figure 13a,) and laser sintering has been used with stainless steel [85,86]. The heat pipes manufactured with LPBF processes generally perform well, and their effective thermal conductivity is significantly higher than the solid material. The ability to produce heat pipes via AM provides many possibilities for electrical machine cooling, as the designs could be fitted for specific needs, and the materials used can be optimized. For example, utilizing off-the-shelf copper heat pipes can lead to increased eddy current and AC losses [87], whereas heat pipes made from electrical steel and integrated directly into an AM machine could provide a significant increase in thermal capabilities without causing appreciable losses.

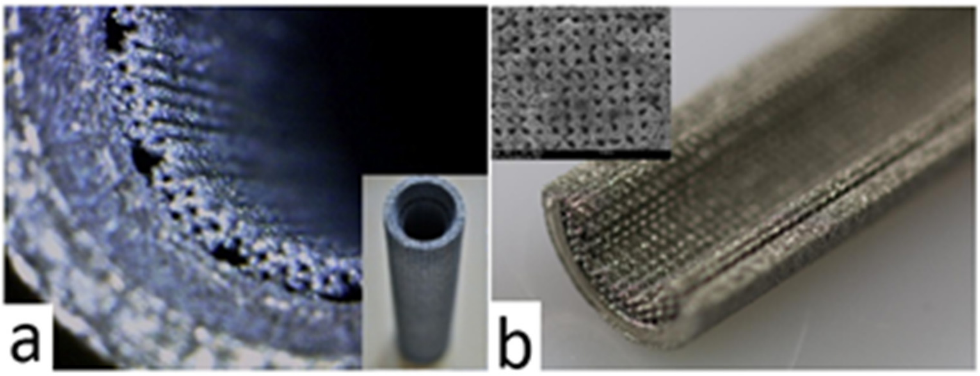

Figure 13. Additively manufactured heat pipes with an internal wick structure (**a**) Reprinted with permission from Ref. [84]. Copyright 2013 Elsevier and (**b**) Reprinted with permission from Ref. [88]. Copyright 2013 Elsevier.

3.4. Direct Conductor Cooling

In a typical machine, most of the heat is generated in the conductors due to Joule losses. The conductors are also the most susceptible to high temperatures due to insulation thermal degradation. While copper is highly thermally conductive, the conductivity of the entire winding body is quite low due to the insulation, air bubble and contact resistances present in windings [89]. Furthermore, in a conventionally cooled machine, the heat needs to travel through the core material, which typically has a low value of thermal conductivity. This creates a large thermal resistance between the windings and the surface of the motor, where the heat can be extracted, leading to high temperatures in the windings. The positive correlation of electrical conductivity with temperature is also notable as it reduces the efficiency of the machine when the conductor temperatures are higher. Due to this, the main challenge when cooling electrical machines is removing heat from the windings.

The thermal resistance between the conductors and the cooling medium can be reduced with the use of direct winding heat exchangers. Liquid-cooled heat exchangers that are in direct contact with the windings have been produced with conventional methods and have shown good results [90,91], although these are difficult to implement, and without AM optimized geometries are difficult to achieve.

An additively manufactured solution was proposed by Wrobel et al. [92], who used SLM to create thermally conductive heat guides from an aluminum alloy (AlSi10Mg), which are designed to be placed between the windings of a motor (Figure 14a). As the heat guides are placed near the windings inside the stator slots, they assist in the heat extraction from the active part of the winding, but also contribute to the machine losses due to eddy currents induced by flux leakage. Therefore, a solid heat guide provides negligible performance improvements, but AM enables the production of different lattice structures (Figure 14b,c) which emulate traditional laminations, and thus, it is possible to eliminate most of the extra losses while keeping a high thermal conductivity. Using a heat guide made with lattice structures, they achieved a 55% increased total thermal conductivity from the winding body of a test motorette without significant extra power losses.

The thermal performance of direct winding heat exchangers can be further increased by utilizing liquid cooling. Sixel et al. [93] created plastic hollow heat exchangers with FDM that allowed for a current density of 20.5 A/mm^2 in the windings. They later improved the design with a lithography-based method to manufacture heat exchangers from alumina ceramic [43] with a measured thermal conductivity of 35 W/m/K (Figure 15a). They achieved a continuous current density of 30.7 A/mm^2 while keeping the maximum winding temperature below 132 C. Using alumina ceramic is noteworthy, as it is both thermally conductive and an electrical insulator, meaning it will not contribute to extra eddy current losses while still not restricting heat flow from the windings to the coolant. To increase the heat transfer from the HE to the liquid coolant, they introduced micro-features on the inside surface of the cooling channel. These increase the total surface area of the HE, albeit at the cost of increased flow resistance and, therefore, higher pumping power. Of the four different solutions considered (Figure 15b), the straight fin design was chosen for its high performance and easy printability.

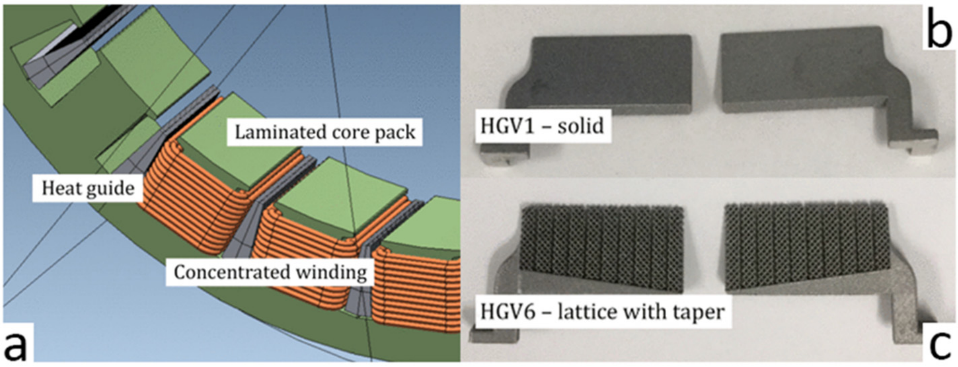

Figure 14. Additively manufactured heat guides places between the windings (**a**), a heat guide with a solid structure (**b**) and a heat guide utilizing a taper and a lattice structure to reduce eddy current losses (**c**) Reprinted with permission from Ref. [92]. Copyright 2020 Elsevier.

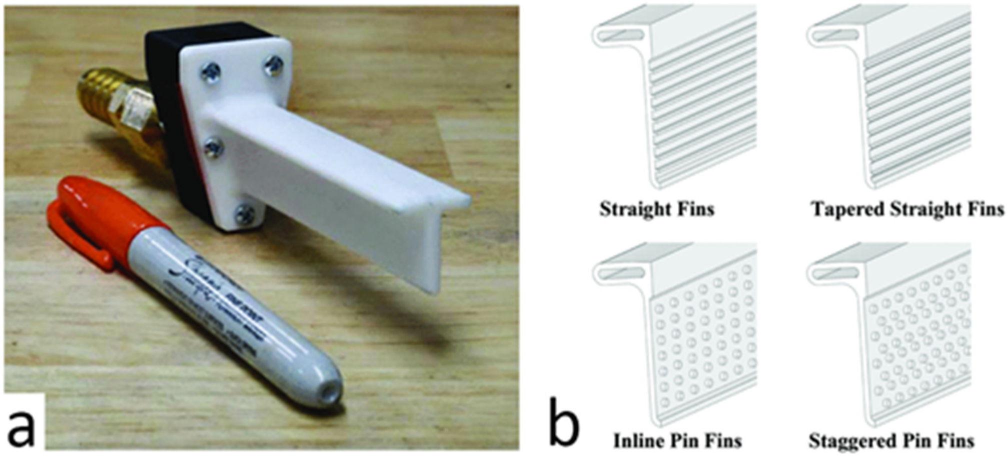

Figure 15. Additively manufactured ceramic heat exchanger for cooling the windings (**a**) and the different types of internal micro-features tested (**b**) Reprinted with permission from Ref. [43]. Copyright 2019 Elsevier.

The additive manufacturing of coil windings directly is also possible. Lorenz et al. [35] have used a multi-material extrusion-based method to create high-performance windings for a switched reluctance machine (Figure 16). The process uses metal or ceramic powders mixed with binding agents to create extrudable pastes, which after heat treatment, achieve suitable physical properties. Although the specific electrical conductivity of this coil is lower at 71% (in part due to the 87% density of the printed material), it excels in thermal performance. One of the reasons for this is the higher thermal conductivity of the ceramic compared to conventional dielectric lacquer (3 vs. 1 W/m/K), which significantly reduces the total thermal resistance of the winding. Another advantage comes from the geometry of the conductor, as any part of the copper is separated from the iron core by just one layer of insulation.

Another possibility to further increase current density is to utilize hollow windings and pump coolant directly inside the conductors. Due to the large conductor dimensions and high costs, this is normally only used for large machines in the 100 MW to GW range [94]. Good results have been achieved with conventionally manufactured coolant conduits wrapped in litz wire [95], but AM looks to be the most promising method for achieving effective hollow conductors for smaller machines.

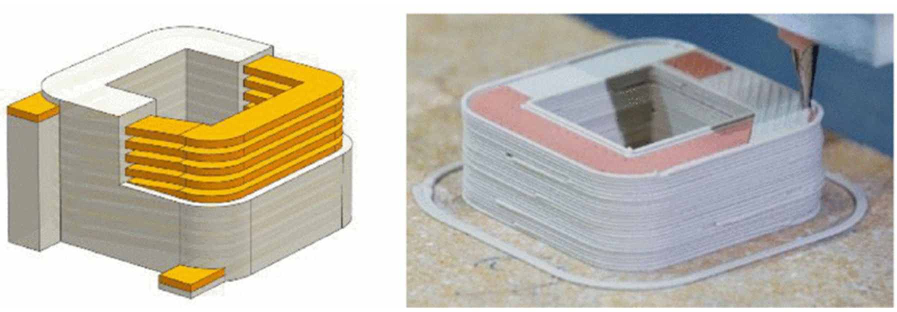

Figure 16. Additively manufactured windings with ceramic insulation for a switched reluctance motor. Reprinted with permission from Ref. [35]. Copyright 2018 Elsevier.

Wohlers et al. [94] have used laser-sintering to create aluminum alloy (AlSi10Mg) fractional-slot concentrated windings, which incorporate a hollow structure for direct liquid cooling of each conductor (Figure 17). In addition to the hollow structure, the rest of the coil geometry is also optimized for minimal losses and maximal cooling. By pumping coolant directly in the conductor, without any interface material (e.g., steel tubes inside the conductors [96]), the thermal resistance between the heat-generating conductors and the coolant is minimized. During testing, the windings were cooled at a constant coolant temperature of 30 °C and achieved a current density of 70 A/mm^2 with a maximum coil temperature of 180 °C. It should be noted that these results are obtained from an aluminum alloy coil and with an identically shaped copper coil, the authors calculate maximum current densities of about 130 A/mm^2.

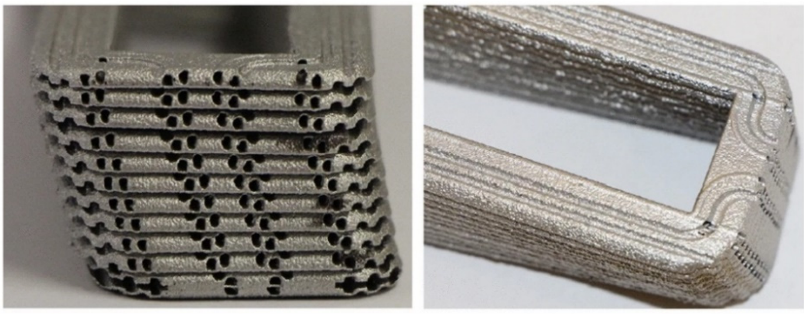

Figure 17. Additively manufactured aluminum alloy windings with a hollow structure for direct conductor water cooling. Reprinted with permission from Ref. [94]. Copyright 2018 Elsevier.

Wu et al. [4] have modelled a similar design (Figure 18a). It uses additively manufactured aluminum alloy (AlSi10Mg) windings and, due to the direct liquid cooling, can achieve a continuous current density of 20 A_{RMS}/mm^2. Continuing their work with hollow conductors, Wu et al. [97] have used DMLS to integrate copper heat pipes in the hollow aluminum alloy windings (Figure 18b). The shape of the windings was also optimized to maximize the filling factor. Adding copper heat pipes inside the conductors creates additional AC losses, but as most of these losses are concentrated in the first winding layers near the slot opening, the authors of the paper proposed a mixed solution, where some conductors don't have heat pipes. Furthermore, in the future, heat pipes may be printed directly in the structure of the windings, which would eliminate the additional AC losses created due to the copper walls of the heat pipe.

Based on the available research work, direct conductor cooling seems to be the most popular method to utilize AM in the thermal management of electrical machines. Since AM provides virtually complete design freedom, it is logical to apply it to solve thermal problems in the most efficient way possible. Additionally, the small features and complex structures required for optimized conductors make it a perfect challenge for AM. Details about the different AM solutions for direct conductor cooling are presented in Table 2.

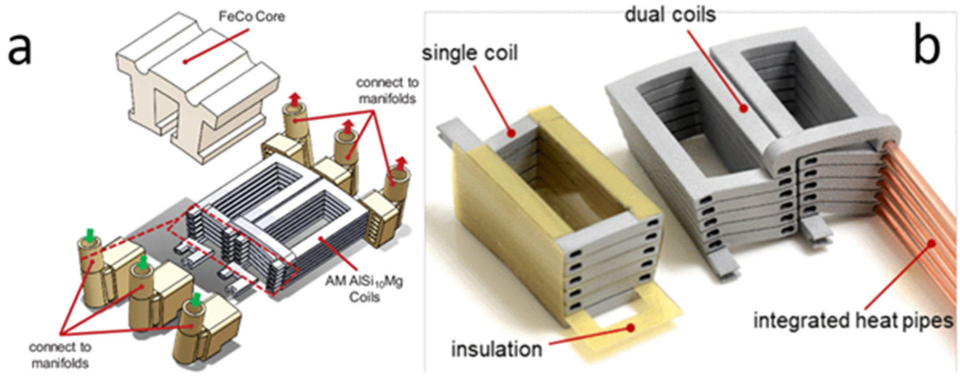

Figure 18. AM (**a**) hollow windings [4] and (**b**) with integrated copper heat pipes reprinted with permission from Ref. [97]. Copyright 2021 Elsevier.

Table 2. Comparison of different AM direct conductor cooling solutions.

AM Direct Winding Cooling Solutions	Method Used	Material Used	Results
Metal Heat Guides [92]	SLM	AlSi10Mg	40% increased input power at lower and 20% at higher excitation frequencies. 55–85% increase of the winding-to-stator thermal conductance. 5% additional power loss at 1 kHz.
Plastic hollow heat exchangers [93]	FDM	Polycarbonate with aluminum flakes	Current density of 20.5 A/mm^2 with non-encapsulated windings while keeping the hotspot temperature below 150 °C
Ceramic hollow heat exchangers [43]	Lithography	Alumina ceramic	Current density of 30.7 A/mm^2 with encapsulated windings while maintaining the hotspot temperature below 132 °C
Additively manufactured SRM windings with ceramic isolation [35]	Paste extrusion	Copper and ceramic powder suspended in paste	Significantly lower temperatures in the conductors due to superior thermal coupling between the winding and stator. Higher temperature tolerance due to the insulation material.
Liquid cooled tooth coil windings [94]	SLS	AlSi10Mg	Current density of 70 A/mm^2 at 180 °C using aluminum coils and a constant 30 °C coolant
Hollow conductor [4]	DMLS	AlSi10Mg	Current density of 20 A/mm^2 at 1.25 kHz using aluminum coils.
Hollow conductor with integrated heat pipe [97]	DMLS	AlSi10Mg	Current density of 13.9 A/mm^2 at 1.25 kHz and 94.34% total motor efficiency using aluminum coils. 7% higher AC losses in the windings due to the electrically conductive heat pipes.

4. Conclusions

Additive manufacturing is successfully pushing the boundaries of design. It allows the production of shapes and structures which have normally been considered impractical or impossible to create. In the field of electrical machines, AM allows the production of complex optimized geometries, which can offer improved electromagnetic and thermal performance. Furthermore, the cost of a part created with AM is not dependent on its complexity, meaning that designers can utilize optimized shapes without needing to worry about manufacturing costs. Finally, the material selection for AM is incredibly wide, with traditional thermally conductive materials such as copper and aluminum being available and less known ceramic materials being used for novel solutions.

Many different solutions for enhancing thermal capabilities with AM have been researched. One of the most common ideas is to use complex lattice structures to create mechanically strong but light structures with very high surface area to increase cooling performance. Another popular solution is to utilize topology optimization to create a highly effective heatsink by balancing surface area with airflow. With multi-objective topology optimization, it is also possible to include mechanical strength and weight in the optimization problem to create a purpose-fit design for specific requirements. Further performance increases can be achieved with heat pipes, which possess extremely high thermal conductivity, and with AM could be seamlessly integrated into existing designs. The list of existing additively manufactured thermal solutions is long, although only a few have been used to cool electrical machines specifically, with most of the research currently focused on demonstrating the usefulness of AM by creating general cooling solutions. This is illustrated in Figure 19 with the maturity levels of different AM thermal management technologies in the context of electrical machines. The two exceptions are AM cooling jackets, which have seen use in industry, but no research on the subject exists, and direct conductor cooling, which has received significant interest and is being actively developed for the purpose of cooling electrical machines specifically.

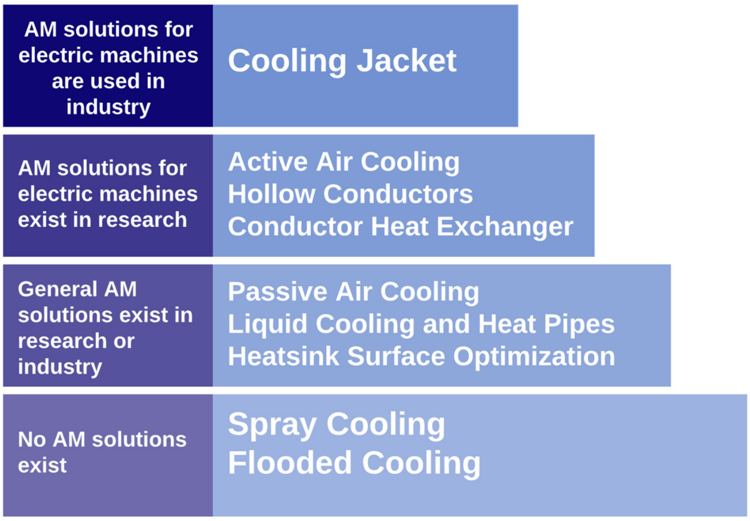

Figure 19. The maturity level of different AM thermal management solutions in the context of cooling electrical machines.

In our opinion, the necessary requirement for additively manufactured electrical machines to be competitive is advanced intra-layer multi-material printing. Currently, the state-of-the-art is dual-metal PBF, which is virtually unexplored in the research field and an obvious direction for future work. An example of utilizing a dual-metal system for enhancing the cooling of electrical machines would be a thermally-conductive frame printed directly on the soft magnetic core, which would eliminate the high thermal resistance usually present in machines with aluminum frames. More advanced multi-material printing would allow the manufacturing of a fully functional machine as a single object. This would need the ability to simultaneously print at least three different materials: a soft magnetic material for the core, a highly conductive material for the windings, and an isolating material to separate the two electrically. When taking into account the current growth of AM technology, it seems likely that this technology will be available in the near future. Moreover, considering the myriad of improvements that a fully AM electrical machine could offer, it could even become the norm for high-performance applications.

In conclusion, the market of additive manufacturing is growing with the amount of industrial applications increasing each year. For electrical machines, AM promises higher power densities through optimized shapes, fast prototyping, and simplified supply chains. Currently, AM is used to produce single components with specific optimizations, but in our opinion, it is only a matter of time when fully additively manufactured electrical machines are commercially viable.

Author Contributions: Conceptualization, M.S., A.K. and P.S.G.; methodology, M.S. and P.S.G.; validation, M.S., A.K. and P.S.G.; writing—original draft preparation, M.S.; writing—review and editing, P.S.G., A.K., H.T. and T.V.; supervision, A.K. and P.S.G. All authors have read and agreed to the published version of the manuscript.

Funding: This research received no external funding.

Institutional Review Board Statement: Not applicable.

Informed Consent Statement: Not applicable.

Data Availability Statement: Not applicable.

Conflicts of Interest: The authors declare no conflict of interest.

References

1. Wohlers Associates. 3D Printing and Additive Manufacturing State of the Industry. 2021. Available online: https://www.fastenernewsdesk.com/28315/wohlers-report-2021-3d-printing-and-additive-manufacturing-global-state-of-the-industry/ (accessed on 25 March 2022).
2. Lux Research. Will 3D Printing Replace Conventional Manufacturing? 2021. Available online: https://parametric-architecture.com/will-3d-printing-technology-replace-traditional-manufacturing/ (accessed on 25 March 2022).
3. Ph.D. Student Wins Additive World Design Challenge Award—Campus News. Available online: https://exchange.nottingham.ac.uk/blog/phd-student-wins-additive-world-design-challenge-award/ (accessed on 21 March 2022).
4. Wu, F.; El-Refaie, A.M. Additively Manufactured Hollow Conductors with Integrated Cooling for High Specific Power Electrical Machines. In Proceedings of the 2020 International Conference on Electrical Machines, ICEM 2020, Gothenburg, Sweden, 23–26 August 2020; pp. 1497–1503. [CrossRef]
5. 3 Additive Manufacturing Technologies to Watch out for in 2017, by 3D Hubs, Xtreme Engineering, Medium. Available online: https://medium.com/extreme-engineering/3-additive-manufacturing-technologies-to-watch-out-for-in-2017-7226d310ca56 (accessed on 16 November 2021).
6. Calignano, F.; Manfredi, D.; Ambrosio, E.P.; Biamino, S.; Lombardi, M.; Atzeni, E.; Salmi, A.; Minetola, P.; Iuliano, L.; Fino, P. Overview on Additive Manufacturing Technologies. *Proc. IEEE* **2017**, *105*, 593–612. [CrossRef]
7. Wohlers, T.; Gornet, T. History of Additive Manufacturing. *Wohlers Rep.* **2014**, *24*, 118.
8. Twotrees. What Is an FDM 3D Printer? How Do FDM 3D Printers Work? Available online: https://twotrees3d.com/fdm-3d-printer-how-do-fdm-3d-printers-work/ (accessed on 31 January 2022).
9. All3DP. The Types of 3D Printing Technology of 2021. Available online: https://all3dp.com/1/types-of-3d-printers-3d-printing-technology/ (accessed on 31 January 2022).
10. 3DPrint.Com. Xerox Unveils ElemX Metal 3D Printer, Collaborates with US Navy. The Voice of 3D Printing/Additive Manufacturing. Available online: https://3dprint.com/278710/xerox-unveils-elemx-metal-3d-printer-with-us-navy-as-first-customer/ (accessed on 31 January 2022).
11. Mostafaei, A.; Elliott, A.M.; Barnes, J.E.; Li, F.; Tan, W.; Cramer, C.L.; Nandwana, P.; Chmielus, M. Binder Jet 3D Printing—Process Parameters, Materials, Properties, Modeling, and Challenges. *Prog. Mater. Sci.* **2021**, *119*, 100707. [CrossRef]
12. Introduction to Binder Jetting 3D Printing, Hubs. Available online: https://www.hubs.com/knowledge-base/introduction-binder-jetting-3d-printing/#what (accessed on 13 February 2022).
13. Weng, Z.; Zhou, Y.; Lin, W.; Senthil, T.; Wu, L. Structure-Property Relationship of Nano Enhanced Stereolithography Resin for Desktop SLA 3D Printer. *Compos. Part A Appl. Sci. Manuf.* **2016**, *88*, 234–242. [CrossRef]
14. Khatri, B.; Lappe, K.; Habedank, M.; Mueller, T.; Megnin, C.; Hanemann, T. Fused Deposition Modeling of ABS-Barium Titanate Composites: A Simple Route towards Tailored Dielectric Devices. *Polymers* **2018**, *10*, 666. [CrossRef] [PubMed]
15. Deckard, C. Method and Apparatus for Producing Parts by Selective Sintering. U.S. Patent 4,863,538A, 17 October 1986.
16. Meiners, W.; Wissenbach, K.; Gasser, A. Shaped Body Especially Prototype or Replacement Part Production. Ger. Patent DE19649865C1, 2 December 1996.
17. Dimensional Accuracy of 3D Printed Parts, Hubs. Available online: https://www.hubs.com/knowledge-base/dimensional-accuracy-3d-printed-parts/#metal (accessed on 16 November 2021).
18. Gong, G.; Ye, J.; Chi, Y.; Zhao, Z.; Wang, Z.; Xia, G.; Du, X.; Tian, H.; Yu, H.; Chen, C. Research Status of Laser Additive Manufacturing for Metal: A Review. *J. Mater. Res. Technol.* **2021**, *15*, 855–884. [CrossRef]
19. Zhang, M.; Zhou, X.; Wang, D.; He, L.; Ye, X.; Zhang, W. Additive Manufacturing of In-Situ Strengthened Dual-Phase AlCoCuFeNi High-Entropy Alloy by Selective Electron Beam Melting. *J. Alloys Compd.* **2022**, *893*, 162259. [CrossRef]
20. McDonough, J.R. A Perspective on the Current and Future Roles of Additive Manufacturing in Process Engineering, with an Emphasis on Heat Transfer. *Therm. Sci. Eng. Prog.* **2020**, *19*, 100594. [CrossRef]
21. Guschlbauer, R.; Burkhardt, A.K.; Fu, Z.; Körner, C. Effect of the Oxygen Content of Pure Copper Powder on Selective Electron Beam Melting. *Mater. Sci. Eng. A* **2020**, *779*, 139106. [CrossRef]

22. Siva Prasad, H.; Brueckner, F.; Volpp, J.; Kaplan, A.F.H. Laser Metal Deposition of Copper on Diverse Metals Using Green Laser Sources. *Int. J. Adv. Manuf. Technol.* **2020**, *107*, 1559–1568. [CrossRef]
23. Ramirez, D.A.; Murr, L.E.; Martinez, E.; Hernandez, D.H.; Martinez, J.L.; MacHado, B.I.; Medina, F.; Frigola, P.; Wicker, R.B. Novel Precipitate–Microstructural Architecture Developed in the Fabrication of Solid Copper Components by Additive Manufacturing Using Electron Beam Melting. *Acta Mater.* **2011**, *59*, 4088–4099. [CrossRef]
24. Guschlbauer, R.; Momeni, S.; Osmanlic, F.; Körner, C. Process Development of 99.95% Pure Copper Processed via Selective Electron Beam Melting and Its Mechanical and Physical Properties. *Mater. Charact.* **2018**, *143*, 163–170. [CrossRef]
25. Jiang, Q.; Zhang, P.; Yu, Z.; Shi, H.; Wu, D.; Yan, H.; Ye, X.; Lu, Q.; Tian, Y. A Review on Additive Manufacturing of Pure Copper. *Coatings* **2021**, *11*, 740. [CrossRef]
26. Ebrahimi, N.D.; Ju, Y.S. Thermal Conductivity of Sintered Copper Samples Prepared Using 3D Printing-Compatible Polymer Composite Filaments. *Addit. Manuf.* **2018**, *24*, 479–485. [CrossRef]
27. Simpson, N.; Mellor, P.H. Additive Manufacturing of Shaped Profile Windings for Minimal AC Loss in Gapped Inductors. In Proceedings of the 2017 IEEE International Electric Machines and Drives Conference, IEMDC 2017, Miami, FL, USA, 21–24 May 2017. [CrossRef]
28. How 3D Printing Is Redefining Inductor Coil Production, GKN Additive. Available online: https://www.gknpm.com/en/our-businesses/gkn-additive/how-3d-printing-is-redefining-inductor-coil-production/ (accessed on 24 January 2022).
29. Wegener, T.; Koopmann, J.; Richter, J.; Krooß, P.; Niendorf, T. CuCrZr Processed by Laser Powder Bed Fusion—Processability and Influence of Heat Treatment on Electrical Conductivity, Microstructure and Mechanical Properties. *Fatigue Fract. Eng. Mater. Struct.* **2021**, *44*, 2570–2590. [CrossRef]
30. METALCOR. CuCr1Zr, C18150, Datasheet. Available online: http://www.metalcor.de/en/datenblatt/133/ (accessed on 24 January 2022).
31. Aboulkhair, N.T.; Simonelli, M.; Parry, L.; Ashcroft, I.; Tuck, C.; Hague, R. 3D Printing of Aluminium Alloys: Additive Manufacturing of Aluminium Alloys Using Selective Laser Melting. *Prog. Mater. Sci.* **2019**, *106*, 100578. [CrossRef]
32. Chen, Z.; Li, Z.; Li, J.; Liu, C.; Lao, C.; Fu, Y.; Liu, C.; Li, Y.; Wang, P.; He, Y. 3D Printing of Ceramics: A Review. *J. Eur. Ceram. Soc.* **2019**, *39*, 661–687. [CrossRef]
33. Rauchenecker, J.; Rabitsch, J.; Schwentenwein, M.; Konegger, T. Additive Manufacturing of Aluminum Nitride Ceramics with High Thermal Conductivity via Digital Light Processing. *Open Ceram.* **2022**, *9*, 100215. [CrossRef]
34. Frigola, P.; Harrysson, O.A.; Horn, T.J.; West, H.A.; Aman, R.L.; Rigsbee, J.M.; Ramirez, D.A.; Murr, L.E.; Medina, F.; Wicker, R.B.; et al. Fabricating Copper Components with Electron Beam Melting. *Adv. Mater. Processes* **2014**, *172*, 20–24.
35. Lorenz, F.; Rudolph, J.; Wemer, R. Design of 3D Printed High Performance Windings for Switched Reluctance Machines. In Proceedings of the 2018 23rd International Conference on Electrical Machines, ICEM 2018, Alexandroupoli, Greece, 3–6 September 2018; pp. 2451–2457. [CrossRef]
36. Buchmayr, B.; Panzl, G.; Walzl, A.; Wallis, C. Laser Powder Bed Fusion—Materials Issues and Optimized Processing Parameters for Tool Steels, AlSiMg- and CuCrZr-Alloys. *Adv. Eng. Mater.* **2017**, *19*, 1600667. [CrossRef]
37. Aluminum 360.0-F Die Casting Alloy. Available online: http://www.matweb.com/search/DataSheet.aspx?MatGUID=46cc3a20683748718693cbb6039bec68 (accessed on 31 January 2022).
38. Sélo, R.R.J.; Catchpole-Smith, S.; Maskery, I.; Ashcroft, I.; Tuck, C. On the Thermal Conductivity of AlSi10Mg and Lattice Structures Made by Laser Powder Bed Fusion. *Addit. Manuf.* **2020**, *34*, 101214. [CrossRef]
39. Krishnan, M.; Atzeni, E.; Canali, R.; Calignano, F.; Manfredi, D.; Ambrosio, E.P.; Iuliano, L. On the Effect of Process Parameters on Properties of AlSi10Mg Parts Produced by DMLS. *Rapid Prototyp. J.* **2014**, *20*, 449–458. [CrossRef]
40. Sarap, M.; Kallaste, A.; Ghahfarokhi, P.S.; Tiismus, H.; Vaimann, T. Determining the Thermal Conductivity of Additively Manufactured Metal Specimens. In Proceedings of the 2022 29th International Workshop on Electric Drives: Advances in Power Electronics for Electric Drives (IWED), Moscow, Russia, 26–29 January 2022.
41. Franco Júnior, A.; Shanafield, D.J. Thermal Conductivity of Polycrystalline Aluminum Nitride (AlN) Ceramics. *Cerâmica* **2004**, *50*, 247–253. [CrossRef]
42. Díaz-Moreno, C.A.; Lin, Y.; Hurtado-Macías, A.; Espalin, D.; Terrazas, C.A.; Murr, L.E.; Wicker, R.B. Binder Jetting Additive Manufacturing of Aluminum Nitride Components. *Ceram. Int.* **2019**, *45*, 13620–13627. [CrossRef]
43. Sixel, W.; Liu, M.; Nellis, G.; Sarlioglu, B. Ceramic 3D Printed Direct Winding Heat Exchangers for Improving Electric Machine Thermal Management. In Proceedings of the 2019 IEEE Energy Conversion Congress and Exposition, ECCE 2019, Baltimore, MD, USA, 29 September–3 October 2019; pp. 769–776. [CrossRef]
44. Urbanek, S.; Frey, P.; Magerkohl, S.; Zimmer, D.; Tasche, L.; Schaper, M.; Ponick, B. Design and Experimental Investigation of an Additively Manufactured PMSM Rotor. In Proceedings of the 2021 IEEE International Electric Machines and Drives Conference, IEMDC 2021, Hartford, CT, USA, 17–20 May 2021. [CrossRef]
45. Application of Additive Manufacturing for Low Torque Ripple of 6/4 Switched Reluctance Motor, IEEE Conference Publication, IEEE Xplore. Available online: https://ieeexplore.ieee.org/document/7837094 (accessed on 16 November 2021).
46. Ibrahim, M.; Bernier, F.; Lamarre, J.M. Novel Multi-Layer Design and Additive Manufacturing Fabrication of a High Power Density and Efficiency Interior PM Motor. In Proceedings of the ECCE 2020—IEEE Energy Conversion Congress and Exposition, Detroit, MI, USA, 11–15 October 2020; pp. 3601–3606. [CrossRef]

47. Tiismus, H.; Kallaste, A.; Vaimann, T.; Rassolkin, A.; Belahcen, A. Additive Manufacturing of Prototype Axial Flux Switched Reluctance Electrical Machine. In Proceedings of the 2021 28th International Workshop on Electric Drives: Improving Reliability of Electric Drives, IWED 2021, Moscow, Russia, 27–29 January 2021. [CrossRef]
48. Wu, S.T.; Huang, P.W.; Chang, T.W.; Jiang, I.H.; Tsai, M.C. Application of Magnetic Metal 3-D Printing on the Integration of Axial-Flow Impeller Fan Motor Design. *IEEE Trans. Magn.* **2021**, *57*, 8201205. [CrossRef]
49. Ge, B.; Ludois, D.C.; Ghule, A.N. A 3D Printed Fluid Filled Variable Elastance Electrostatic Machine Optimized with Conformal Mapping. In Proceedings of the ECCE 2016—IEEE Energy Conversion Congress and Exposition, Milwaukee, WI, USA, 18–22 September 2016. [CrossRef]
50. Aconity MIDI+, Aconity3D. Available online: https://aconity3d.com/products/aconity-midi-plus/ (accessed on 16 November 2021).
51. Kallaste, A.; Vaimann, T.; Rassalkin, A. Additive Design Possibilities of Electrical Machines. In Proceedings of the 2018 IEEE 59th Annual International Scientific Conference on Power and Electrical Engineering of Riga Technical University, RTUCON 2018, Riga, Latvia, 12–13 November 2018. [CrossRef]
52. Topology Optimization—An Overview, ScienceDirect Topics. Available online: https://www.sciencedirect.com/topics/computer-science/topology-optimization (accessed on 17 November 2021).
53. Abdalmagid, M.; Sayed, E.; Bakr, M.; Emadi, A. Geometry and Topology Optimization of Switched Reluctance Machines: A Review. *IEEE Access* **2022**, *10*, 5141–5170. [CrossRef]
54. Zhu, J.; Zhou, H.; Wang, C.; Zhou, L.; Yuan, S.; Zhang, W. A Review of Topology Optimization for Additive Manufacturing: Status and Challenges. *Chin. J. Aeronaut.* **2021**, *34*, 91–110. [CrossRef]
55. Misiun, G.; van de Ven, E.; Langelaar, M.; Geijselaers, H.; van Keulen, F.; van den Boogaard, T.; Ayas, C. Topology Optimization for Additive Manufacturing with Distortion Constraints. *Comput. Methods Appl. Mech. Eng.* **2021**, *386*, 114095. [CrossRef]
56. Topology Optimization for 3D Printing—3Dnatives. Available online: https://www.3dnatives.com/en/topology-optimisation140820184/ (accessed on 17 November 2021).
57. Langelaar, M. Topology Optimization of 3D Self-Supporting Structures for Additive Manufacturing. *Addit. Manuf.* **2016**, *12*, 60–70. [CrossRef]
58. Walton, D.; Moztarzadeh, H. Design and Development of an Additive Manufactured Component by Topology Optimisation. *Procedia CIRP* **2017**, *60*, 205–210. [CrossRef]
59. Gaynor, A.T.; Meisel, N.A.; Williams, C.B.; Guest, J.K. Multiple-Material Topology Optimization of Compliant Mechanisms Created Via PolyJet Three-Dimensional Printing. *J. Manuf. Sci. Eng.* **2014**, *136*, 061015. [CrossRef]
60. Lazarov, B.S.; Sigmund, O.; Meyer, K.E.; Alexandersen, J. Experimental Validation of Additively Manufactured Optimized Shapes for Passive Cooling. *Appl. Energy* **2018**, *226*, 330–339. [CrossRef]
61. Wits, W.W.; Jafari, D.; Jeggels, Y.; van de Velde, S.; Jeggels, D.; Engelberts, N. Freeform-Optimized Shapes for Natural-Convection Cooling. In Proceedings of the Therminic 2018—24th International Workshop on Thermal Investigations of ICs and Systems, Stockholm, Sweden, 26–28 September 2018. [CrossRef]
62. Helou, M.; Kara, S. Design, Analysis and Manufacturing of Lattice Structures: An Overview. *Int. J. Comput. Integr. Manuf.* **2017**, *31*, 243–261. [CrossRef]
63. Kovalevsky, A.; Mats, A.; Shmurak, M.; Fleisher, A. Experimental Study of Aluminum Foams Thermal Conductivity. Prospects of Additive Manufacturing for Novel Heat Exchangers Production. In Proceedings of the 2020 IEEE 10th International Conference on Nanomaterials: Applications and Properties, NAP 2020, Sumy, Ukraine, 9–13 November 2020. [CrossRef]
64. Wang, N.; Kaur, I.; Singh, P.; Li, L. Prediction of Effective Thermal Conductivity of Porous Lattice Structures and Validation with Additively Manufactured Metal Foams. *Appl. Therm. Eng.* **2021**, *187*, 116558. [CrossRef]
65. Takezawa, A.; Zhang, X.; Kitamura, M. Optimization of an Additively Manufactured Functionally Graded Lattice Structure with Liquid Cooling Considering Structural Performances. *Int. J. Heat Mass Transf.* **2019**, *143*, 118564. [CrossRef]
66. Yang, L.; Mertens, R.; Ferrucci, M.; Yan, C.; Shi, Y.; Yang, S. Continuous Graded Gyroid Cellular Structures Fabricated by Selective Laser Melting: Design, Manufacturing and Mechanical Properties. *Mater. Des.* **2019**, *162*, 394–404. [CrossRef]
67. Kaur, I.; Singh, P. Critical Evaluation of Additively Manufactured Metal Lattices for Viability in Advanced Heat Exchangers. *Int. J. Heat Mass Transf.* **2021**, *168*, 120858. [CrossRef]
68. Smith, R. *Thermal Testing of a 3D Printed Super Dense Mesh Heatsink against State-of-The-Art Finned Geometry*; Qualified Rapid Products: West Jordan, UT, USA, 2015.
69. Wong, M.; Owen, I.; Sutcliffe, C.J.; Puri, A. Convective Heat Transfer and Pressure Losses across Novel Heat Sinks Fabricated by Selective Laser Melting. *Int. J. Heat Mass Transf.* **2009**, *52*, 281–288. [CrossRef]
70. Wrobel, R.; Scholes, B.; Mustaffer, A.; Ullah, S.; Reay, D.; Mecrow, B.; Hussein, A. Design and Experimental Characterisation of an Additively Manufactured Heat Exchanger for the Electric Propulsion Unit of a High-Altitude Solar Aircraft. In Proceedings of the 2019 IEEE Energy Conversion Congress and Exposition, ECCE 2019, Baltimore, MD, USA, 29 September–3 October 2019; pp. 753–760. [CrossRef]
71. Rao, Y.; Li, B.; Feng, Y. Heat Transfer of Turbulent Flow over Surfaces with Spherical Dimples and Teardrop Dimples. *Exp. Therm. Fluid Sci.* **2015**, *61*, 201–209. [CrossRef]
72. Ventola, L.; Robotti, F.; Dialameh, M.; Calignano, F.; Manfredi, D.; Chiavazzo, E.; Asinari, P. Rough Surfaces with Enhanced Heat Transfer for Electronics Cooling by Direct Metal Laser Sintering. *Int. J. Heat Mass Transf.* **2014**, *75*, 58–74. [CrossRef]

73. Kirsch, K.L.; Thole, K.A. Pressure Loss and Heat Transfer Performance for Additively and Conventionally Manufactured Pin Fin Arrays. *Int. J. Heat Mass Transf.* **2017**, *108*, 2502–2513. [CrossRef]
74. European Powder Metallurgy Association (EPMA). Cooling Jacket with Internal Helix Structure. Available online: https://www.epma.com/spotlight-on-pm/cooling-jacket-with-internal-helix-structure (accessed on 10 February 2022).
75. Additive Manufactured Electric Motor. Available online: https://ncam.the-mtc.org/case-studies/additive-manufactured-electric-motor/ (accessed on 11 February 2022).
76. Kim, J.; Yoo, D.J. 3D Printed Compact Heat Exchangers with Mathematically Defined Core Structures. *J. Comput. Des. Eng.* **2020**, *7*, 527–550. [CrossRef]
77. Kaur, I.; Singh, P. State-of-the-Art in Heat Exchanger Additive Manufacturing. *Int. J. Heat Mass Transf.* **2021**, *178*, 121600. [CrossRef]
78. Moon, H.; Miljkovic, N.; King, W.P. High Power Density Thermal Energy Storage Using Additively Manufactured Heat Exchangers and Phase Change Material. *Int. J. Heat Mass Transf.* **2020**, *153*, 119591. [CrossRef]
79. Bernardin, J.D.; Ferguson, K.; Sattler, D. The Testing and Model Validation of an Additively Manufactured Twisted Tube Heat Exchanger. In Proceedings of the ASME 2019 13th International Conference on Energy Sustanability, Collocated with the ASME 2019 Heat Transfer Summer Conference, Bellevue, WA, USA, 14–17 July 2019. [CrossRef]
80. Putra, N.; Ariantara, B. Electric Motor Thermal Management System Using L-Shaped Flat Heat Pipes. *Appl. Therm. Eng.* **2017**, *126*, 1156–1163. [CrossRef]
81. Chaudhry, H.N.; Hughes, B.R.; Ghani, S.A. A Review of Heat Pipe Systems for Heat Recovery and Renewable Energy Applications. *Renew. Sustain. Energy Rev.* **2012**, *16*, 2249–2259. [CrossRef]
82. Thompson, S.M.; Aspin, Z.S.; Shamsaei, N.; Elwany, A.; Bian, L. Additive Manufacturing of Heat Exchangers: A Case Study on a Multi-Layered Ti–6Al–4V Oscillating Heat Pipe. *Addit. Manuf.* **2015**, *8*, 163–174. [CrossRef]
83. Esarte, J.; Blanco, J.M.; Bernardini, A.; San-José, J.T. Optimizing the Design of a Two-Phase Cooling System Loop Heat Pipe: Wick Manufacturing with the 3D Selective Laser Melting Printing Technique and Prototype Testing. *Appl. Therm. Eng.* **2017**, *111*, 407–419. [CrossRef]
84. Ameli, M.; Agnew, B.; Leung, P.S.; Ng, B.; Sutcliffe, C.J.; Singh, J.; McGlen, R. A Novel Method for Manufacturing Sintered Aluminium Heat Pipes (SAHP). *Appl. Therm. Eng.* **2013**, *52*, 498–504. [CrossRef]
85. Ozguc, S.; Pai, S.; Pan, L.; Geoghegan, P.J.; Weibel, J.A. Experimental Demonstration of an Additively Manufactured Vapor Chamber Heat Spreader. In Proceedings of the 18th InterSociety Conference on Thermal and Thermomechanical Phenomena in Electronic Systems, ITHERM 2019, Las Vegas, NV, USA, 28–31 May 2019; pp. 416–422. [CrossRef]
86. Richard, B.; Pellicone, D.; Anderson, W.G. Loop Heat Pipe Wick Fabrication via Additive Manufacturing. In Proceedings of the 47th International Conference on Environmental Systems, Charleston, SC, USA, 16–20 July 2017.
87. Wrobel, R.; Reay, D. A Feasibility Study of Heat Pipes for Thermal Management of Electrical Machines. In Proceedings of the ECCE 2020—IEEE Energy Conversion Congress and Exposition, Detroit, MI, USA, 11–15 October 2020; pp. 4230–4237. [CrossRef]
88. McGlen, R.J. An Introduction to Additive Manufactured Heat Pipe Technology and Advanced Thermal Management Products. *Therm. Sci. Eng. Prog.* **2021**, *25*, 100941. [CrossRef]
89. Chong, Y.C.; Staton, D.; Gai, Y.; Adam, H.; Popescu, M. Review of Advanced Cooling Systems of Modern Electric Machines for Emobility Application. In Proceedings of the 2021 IEEE Workshop on Electrical Machines Design, Control and Diagnosis, WEMDCD 2021, Modena, Italy, 8–9 April 2021; pp. 149–154. [CrossRef]
90. Semidey, S.A.; Mayor, J.R. Experimentation of an Electric Machine Technology Demonstrator Incorporating Direct Winding Heat Exchangers. *IEEE Trans. Ind. Electron.* **2014**, *61*, 5771–5778. [CrossRef]
91. Schiefer, M.; Doppelbauer, M. Indirect Slot Cooling for High-Power-Density Machines with Concentrated Winding. In Proceedings of the 2015 IEEE International Electric Machines and Drives Conference, IEMDC 2015, Coeur d'Alene, ID, USA, 10–13 May 2015; pp. 1820–1825. [CrossRef]
92. Wrobel, R.; Hussein, A. A Feasibility Study of Additively Manufactured Heat Guides for Enhanced Heat Transfer in Electrical Machines. *IEEE Trans. Ind. Appl.* **2020**, *56*, 205–215. [CrossRef]
93. Sixel, W.; Liu, M.; Nellis, G.; Sarlioglu, B. Cooling of Windings in Electric Machines via 3-D Printed Heat Exchanger. *IEEE Trans. Ind. Appl.* **2020**, *56*, 4718–4726. [CrossRef]
94. Wohlers, C.; Juris, P.; Kabelac, S.; Ponick, B. Design and Direct Liquid Cooling of Tooth-Coil Windings. *Electr. Eng.* **2018**, *100*, 2299–2308. [CrossRef]
95. Lindh, P.; Petrov, I.; Jaatinen-Varri, A.; Gronman, A.; Martinez-Iturralde, M.; Satrústegui, M.; Pyrhonen, J. Direct Liquid Cooling Method Verified with an Axial-Flux Permanent-Magnet Traction Machine Prototype. *IEEE Trans. Ind. Electron.* **2017**, *64*, 6086–6095. [CrossRef]
96. Polikarpova, M.; Ponomarev, P.; Röyttä, P.; Semken, S.; Alexandrova, Y.; Pyrhönen, J. Direct Liquid Cooling for an Outer-Rotor Direct-drive Permanent-Magnet Synchronous Generator for Wind Farm Applications. *IET Electr. Power Appl.* **2015**, *9*, 523–532. [CrossRef]
97. Wu, F.; El-Refaie, A.; Al-Qarni, A. Additively Manufactured Hollow Conductors Integrated with Heat Pipes: Design Tradeoffs and Hardware Demonstration. *IEEE Trans. Ind. Appl.* **2021**, *57*, 3632–3642. [CrossRef]